energies

MDPI

Article

Development and Evaluation of Large-Size Phase Change Proppants for Fracturing of Marine Natural Gas Hydrate Reservoirs

Zhanqing Qu [1], Jiacheng Fan [1,*], Tiankui Guo [1], Xiaoqiang Liu [2], Jian Hou [1] and Meijia Wang [3]

[1] School of Petroleum Engineering, China University of Petroleum (East China), Qingdao 266580, China
[2] Beijing International Gas Hydrate Research Center, Peking University, Beijing 100871, China
[3] Sinopec Shengli Oilfield Xianhe Oil Production Plant Technology Institute, Dongying 257000, China
* Correspondence: 15589840609@163.com

Abstract: The stimulation method of the marine natural gas hydrate (NGH) reservoir through hydraulic fracturing has been proposed to resolve the problem of the low production capacity in the conventional development method of pressure drawdown. Nevertheless, due to the strong plasticity and high argillaceous siltstone content of the marine NGH reservoir, conventional small-particle-size proppant cannot form effective support for fractures after fracturing because of serious embedding in the reservoir. To solve this problem, the large-size phase change proppants were developed in this study. First, an epoxy resin curing system that can reduce curing time to 40 min in low temperature and humid environment was developed. Then, the epoxy resin and curing system was emulsified, and through the optimization of the emulsification process, the particle size of the proppant can be controlled in 0.5–4.5 mm and the cementation between the proppant particles during the curing process can be prevented. Finally, the proppant performances were evaluated. The performance evaluation shows that the cured proppants have regular structure and good compressive strength, and the emulsion proppants have good transport capacity. Their large sizes provide effective propping effects for fractures generated in weakly cemented clayey silt marine NGH reservoirs.

Keywords: natural gas hydrate; hydraulic fracturing; large size phase change proppant; low-temperature curing agent; performance evaluation

Citation: Qu, Z.; Fan, J.; Guo, T.; Liu, X.; Hou, J.; Wang, M. Development and Evaluation of Large-Size Phase Change Proppants for Fracturing of Marine Natural Gas Hydrate Reservoirs. *Energies* **2022**, *15*, 8018. https://doi.org/10.3390/en15218018

Academic Editor: Reza Rezaee

Received: 13 September 2022
Accepted: 21 October 2022
Published: 28 October 2022

1. Introduction

The NGH is a kind of ice-like crystalline compound of gas and water formed in a low-temperature and high-pressure environment, and it has become a promising clean energy with its rich reserves, high combustion efficiency and less environmental pollution [1]. Currently, the NGH is developed by the pressure drawdown method, and this method has the disadvantage of the limited swept range of the bottom hole pressure drop. An efficient seepage channel for the decomposed NGH is the key to enlarging the swept range of the bottom hole pressure drop and increasing the development efficiency, and this can be realized by hydraulic fracturing, where the fractures are generated in the reservoir and propped by the proppants [2]. For the weakly cemented NGH reservoirs stored in the seafloor surface sediments, the reservoir shows strong plasticity, which causes serious embedding of conventional small, solid proppants within fractures, and the generated fractures cannot be propped effectively [3]. Conventional large-size solid proppants such as quartz sand and ceramsite cannot be migrated to remote fractures because of their large mass and the friction caused by contact between the particles during the migration process because of the irregular surface, and proppant particles with large particle size and rigid structure are also likely to cause plugging of distal fractures and branch fractures. To improve the development efficiency and simplify the construction process of hydraulic fracturing in marine NGH reservoirs, a new type of large-particle-size phase change

proppant that can be carried directly by the fracturing fluid and has good migration ability was developed.

At present, three types of phase change proppants are most commonly mentioned: small molecular gels, supramolecular polymers and emulsified epoxy resins. The small molecule gel refers to an organic molecule with a molecular weight below 2000. Under environmental stimulation, organic molecules form strong structures through non-covalent interactions between molecules [4]. Supramolecular gels are based on the formation of aggregates by low-molecular-weight gelling factors through non-covalent interactions, and further entangle the aggregates to obtain a three-dimensional structure [5]. Emulsified thermosetting epoxy resin is used to mix and emulsify thermosetting resin and its curing agent to obtain emulsions with different droplet sizes. Under the stimulation of reservoir temperature, the resin and curing agent are cured in the droplets and proppants with different particle sizes are obtained.

Pei investigated three existing systems of phase change proppants to analyze their defects and performance advantages. A new-type self-propping frac fluid was developed through gelation of a kind of small molecule gel by heating. The phase change liquid is carried by frac fluid and injected into the post-frac reservoir. Its transformed temperature is 85 °C, and the particle size is distributed in a range from 20/40 mesh to 40/70 mesh; it is uncontrollable [6]. A new type of phase change proppants suitable for a 60–90 °C reservoir was developed though a liquid–solid phase transition of supramolecular materials subject to temperature increase. The effect of proppants generation in the reservoir environment was evaluated and it was found that the proppant particles formed under static conditions are large and irregular in shape [7]. One kind of phase change proppants was developed based on bisphenol-A epoxy resin emulsion. The proppant particle size is mainly distributed between 30 mesh and 50 mesh, and the proppants have good compressive strength and regular morphology [8].

The existing phase change proppant systems usually have small sizes, which cannot meet the requirements of fracture propping in the NGH reservoir. The phase change proppant based on supramolecular polymer and small molecule gel only occur at the high temperature, and cannot be applicable in the NGH reservoir with the low temperature. The resin emulsion system has limitations in the low curing rate at low temperature and the tendency of particle agglomerate when proppants are generated in the static conditions in the reservoir. To make the obtained proppant particles have regular morphology and controllable particle size, emulsified resin system is selected for the development of large-particle-size phase change proppants. First, through the synthesis of a new polythiol curing agent and its compounding with amine curing agent, a fast-curing agent system for epoxy resin suitable for low temperature and humidity environment was obtained. Then, by optimizing the type of emulsifier and the emulsification process, a large-particle-size phase change proppant with controllable particle size is obtained, and the surface treatment of the emulsion droplets prevents the cementation between proppant particles during the curing process. Finally, evaluation is conducted of the obtained large-particle-size phase change proppant. Through the evaluation test, it is found that the obtained large-size phase change proppant has good migration ability, and the proppant particles can still form an effective seepage channel in the seriously embedded hydrate reservoir, which can meet the development needs of the marine NGH reservoirs.

2. Development of the Large-Size Resin Phase Change Proppants

2.1. Materials

The proppants were synthesized with materials such as dimethyl sulfoxide, glycerol, mercaptopropionic acid and concentrated sulfuric acid obtained from Sinopharm Group Chemical Reagent Co., Ltd. (Shanghai, China). Hollow glass microspheres and silica particles with diameters of 100 nm, 0.01 μm, 0.1 μm and 1 μm were obtained from Zhongke Yanuo New Material Technology Co., Ltd. (Beijing, China). The proppant performances

were evaluated with the guar gum frac fluid, quartz sand and ceramsite proppants, which were obtained from Shengli Oilfield (Shandong, China).

2.2. Synthesis and Characterization of Polythiol Curing Agents

The polythiol curing agent has two or more sulfhydryl groups at its structure terminal. Due to the high density of the existing polythiol curing agent [9]. To improve the migration ability of the obtained proppant system, a new low-density ester polythiol curing agent was synthesized. In the synthesis experiment, glycerol and mercaptopropionic acid with a mole ratio of 1:3 were selected as the reactive monomer, and dimethyl sulfoxide was used as the solvent. First, the glycerol was dissolved in the dimethyl sulfoxide and was stirred evenly, and the strong sulfuric acid with a mass concentration of 10% was added as the catalyst and dehydrant. Then, the thioglycolic acid was added for esterification reaction at a temperature of 70 °C and stirred for 6 h at a constant temperature [10]. Finally, the synthetic product was precipitated in a saturated sodium bicarbonate solution, and the sediment was dried to obtain the target polythiol curing agent. The product of the synthesis reaction is the white waxy solid, which is not water soluble. The reaction formula and product morphology are shown in Figures 1 and 2.

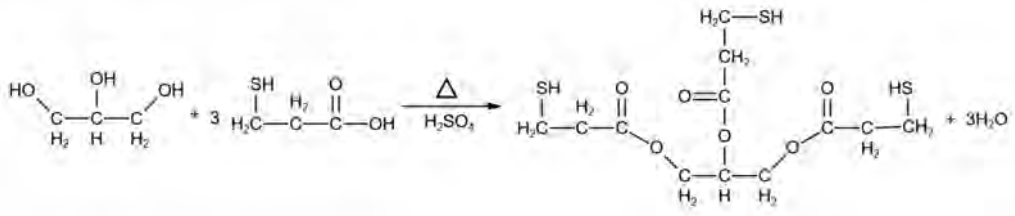

Figure 1. Synthesis reaction formula of polythiol curing agent.

Figure 2. Synthetic product morphology.

2.3. Optimization of Compound Curing Agent System

Considering that the marine NGH is generally formed at a temperature lower than 10 °C, the curing experiment was operated in a water circumstance at 5 °C [11]. The resin used in the experiment is a low-density epoxy resin (1.2 g/cm^3) based on eugenol, and hollow glass microspheres with 1.5% of the resin mass are added to reduce the density to about 1 g/cm^3, which can be effectively suspended in the carrier liquid. As the polythiol curing agent is reacted with the tertiary amines as an accelerator, the polythiol is compound with a tertiary amine curing agent (adduct of diethylene triamine and butyl glycidyl ether) with a certain curing capability in a wet environment, and the curing capability is evaluated by measuring the complete curing time. The applicable compound system is optimized by determining the curing time after changing the ratio, and the final proppant system meets the requirements of proppant curing in the marine NGH reservoir. The results of the evaluation experiments are shown in Table 1.

Table 1. Curing time of curing agent system with different proportions.

No	Dosage of Polythiol Curing Agent/%	Amine Curing Accelerator Dosage/%	Fully Cure Time/min
1	100	0	124
2	90	10	92
3	80	20	69
4	70	30	42
5	60	40	38
6	50	50	49
7	40	60	63
8	30	70	84
9	20	80	96
10	10	90	107
11	0	100	116

It can be seen from the results of the curing experiment that the curing time of using only polythiol or amine curing agent in a low temperature and humid environment is 124 min and 116 min, respectively. As there is currently no fracturing production for NGH reservoirs, combined with conventional reservoir fracturing development technology, the fracture closure time is usually less than 60 min, so the use of these two curing agents alone cannot meet the needs of NGH reservoir development [12]. When the two curing agents are used in combination, because of the accelerating effect of the amine curing agent on the polythiol curing agent and the exothermic reaction of the amine curing agent with the epoxy resin to accelerate the reaction rate, the curing time is significantly shortened. When the mass ratio of the polythiol curing agent and amine curing agent is 6:4, the curing time is shortened to less than 40 min, which allows the proppant in the emulsion phase to solidify before the fracture is closed, thus effectively propping the fracture.

2.4. Selection of Emulsifiers and Emulsification Mechanism Analysis

2.4.1. Selection of the Type of Emulsifier

The oil-in-water surfactant emulsifier of sodium dodecyl benzene sulfonate (SDBS) and the hydrophilic SiO_2 particles with irregular morphology and particle size of 0.01 μm were selected as emulsifiers to prepare the emulsion proppant. The amount of emulsifier is 1% of the resin mass and it is excessive [13]. The emulsification was operated at the stirring rate of 200 rpm by adding ethanol to the resin as an inert diluent, and the mass ratio of the curing system and resin is 1:4. The emulsifier type was optimized by evaluating the microstructure of proppant particles through SEM observation and the mechanism of different emulsifier types was analyzed. The microscopic and surface morphologies of the cured proppants obtained by using surfactant emulsifier (SDBS) and SiO_2 particles as emulsifiers are shown in Figure 3.

Compared with the cured proppants generated with surfactant emulsifier, the proppant produced with this solid-particle emulsifier has a large size, regular structure, and flat surface. This is because the adsorption of surfactant emulsifier at the oil–water interface is reversible, and the dynamic balance of adsorption and desorption forms a stable emulsion. During resin curing, the resin viscosity is increased, and equilibrium of the active emulsifier adsorption and desorption is destroyed, which changes the emulsion stability [14]. The hydrophilic solid particle maintains the emulsion stability with two mechanisms. First, the block-shaped particles are adsorbed irreversibly on the oil–water as the mechanical barrier, and the flake-shaped particles form the 3D network as the continuous phase. This structure not only reduces the mobility of the emulsion droplets, but also prevents them from influencing the environment during the reaction between the oil phase and the curing agent (Figure 4). Second, the three-phase contact angle of hydrophilic particles is less than 90° ($\theta < 90°$), which means that a small part of the particles is submerged in the oil phase, and most of the particles are submerged in the water phase (Figure 5), which improves the coverage of solid particles on the oil–phase surface [15]. The hydrophilic solid particles are

optimized as the emulsifier for the phase change proppant system, and the hydrophilic SiO_2 solid particles are selected considering application cost and environmental friendliness.

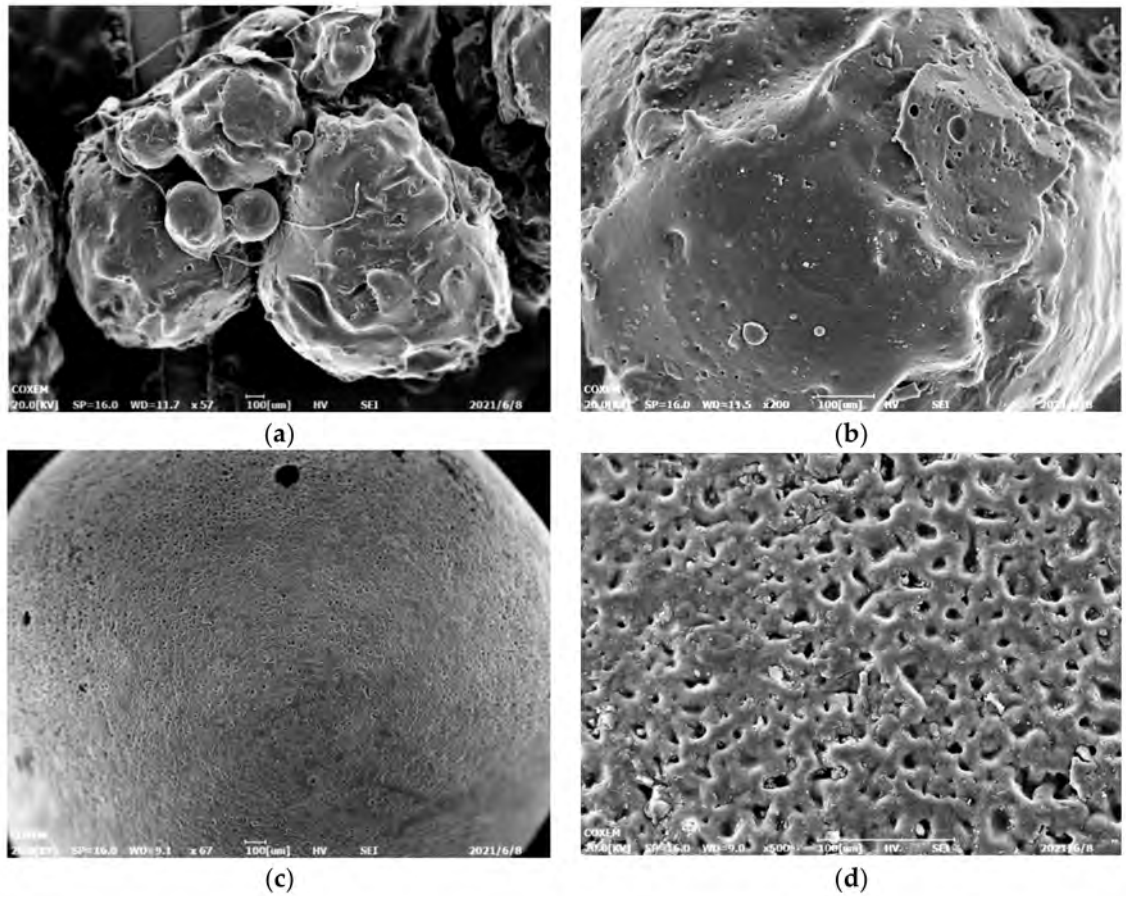

Figure 3. Proppant particles and surface morphology obtained from sodium dodecyl benzene sulfonate and solid particle emulsifier. ((**a**,**b**) are the proppant particles and surface morphology obtained from sodium dodecylbenzene sulfonate; (**c**,**d**) are the proppant particles and surface morphology obtained from solid particle emulsifier.)

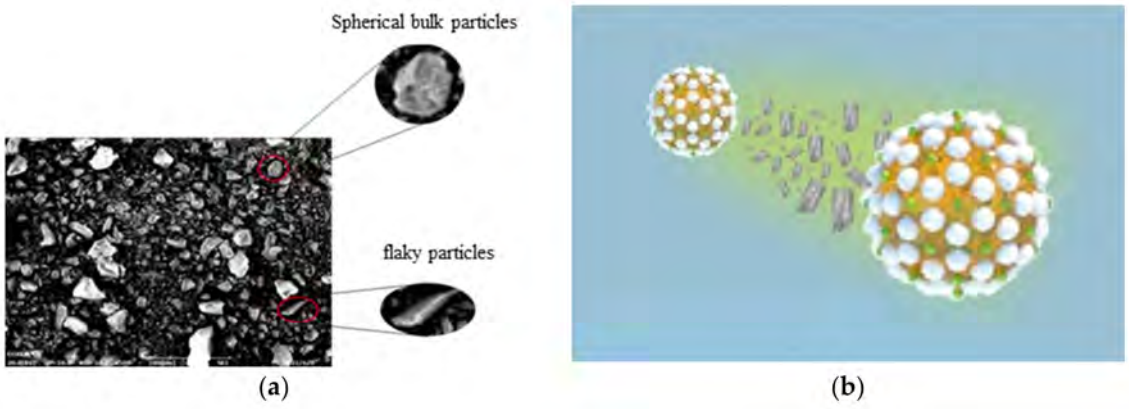

Figure 4. Microscopic morphology of SiO_2 particles and mechanism of emulsion stabilization. (**a**) is the microscopic morphology of SiO_2 particles; (**b**) is the mechanism of emulsion stabilization of SiO_2 particles.

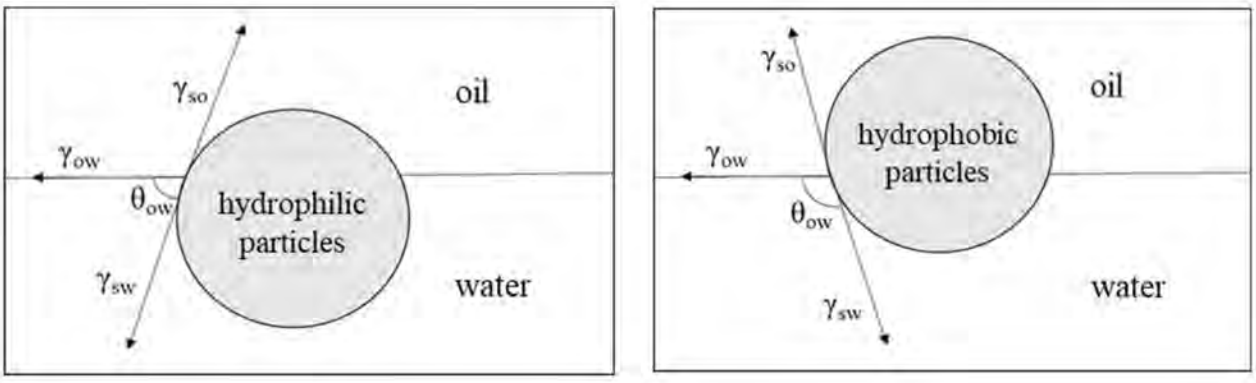

Figure 5. Adsorption state of hydrophilic and hydrophobic particles at the oil–water interface.

2.4.2. Optimal Particle Size of Emulsifier

The energy E required for particles to be separated from the oil–water interface is expressed as [16]:

$$E = -\Delta_{int}G = \pi R^2 \gamma_{ow}(1 \pm \cos\theta)^2 \quad (1)$$

where θ is the contact angle among particle, oil and water, γ_{ow} is the oil–water interfacial tension, the particle gravity is ignored considering the uniform sphere and small-enough size of particles and R is the diameter of a single spherical particle.

The emulsifier particle size has a greater effect on the emulsion performance. Under the same emulsifier concentration, the emulsion droplet size increases with an increase in emulsifier particles size. Nevertheless, in practical application, when the emulsifier particle size reaches a value, the sedimentation rate of the emulsifier particles increases, and the emulsification stability reduces, which lead to less uniformity of the droplet size [17]. To make the size of the obtained proppant meet the production requirements of NGH reservoirs, SiO_2 particles with particle diameters of 0.01 μm, 0.05 μm and 0.1 μm were taken as emulsifiers. The amount of emulsifier is 1% of the resin mass, adding the ethanol with a concentration of 20% as the diluter and then mixing and stirring them at the rate of 200 rpm. The emulsion was prepared, and the proppant particle size distribution was analyzed. The results are illustrated in Figure 6.

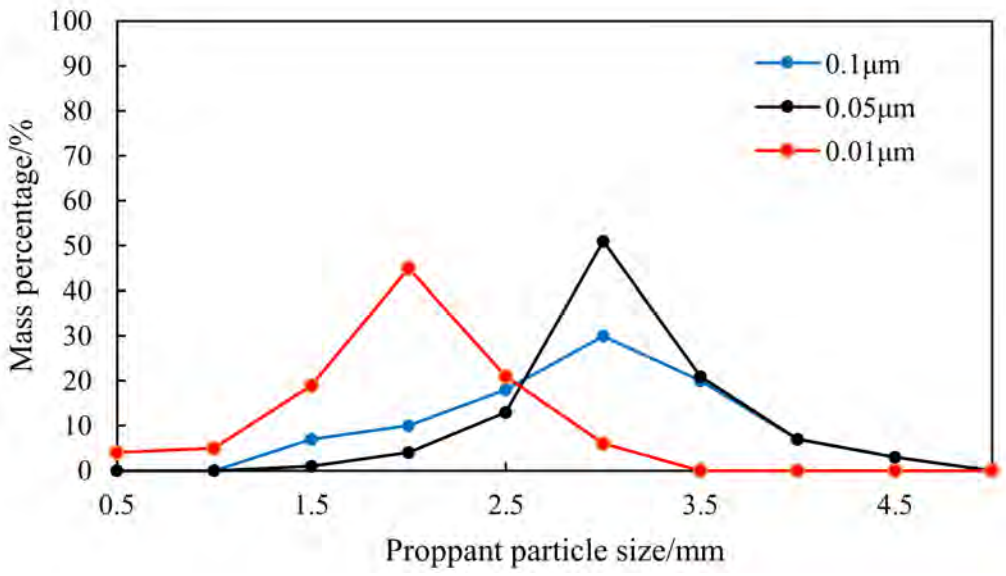

Figure 6. Particle size distribution of proppant obtained from different SiO_2 particles sizes.

According to the evaluation results, the proppant particles obtained from 0.01 μm and 0.05 μm SiO_2 particles are mainly distributed in 2 mm and 3 mm, respectively, and their mass proportions are 45% and 51%. The proppant made from 0.05 μm SiO_2 particles has a larger particle size. When the SiO_2 size increased to 0.1 μm, the mass proportions of the obtained proppant particles at 2.5 mm, 3 mm and 3.5 mm were 18%, 30% and 20%, respectively, and the particle size uniformity of the proppant decreased. Comparison shows that the proppants generated with 0.05 μm SiO_2 as the emulsifier has the larger sizes and more uniform distribution than those generated with 0.01 μm SiO_2 and 0.1 μm SiO_2 as the emulsifier. Considering that the strong plasticity of the NGH reservoir causes serious proppant embedding, and the large-size proppants are needed to prop the fracture, so the 0.05 μm SiO_2 particles are selected as the emulsifier.

Combined with the selected synthetic raw materials and emulsion preparation materials, the cost per cubic meter of phase change proppants is about RMB 1400, which is twice that of quartz sand proppant and lower than that of ceramic proppants. The cost can meet the requirements of a large number of applications in the mining process.

2.5. Controllable Treatment of Proppant Particle Size

Through experiments, it is found that the change of the emulsifier concentration mainly affects the coverage of the emulsifier on the surface of the emulsion droplets and has little effect on the particle size of the obtained proppant. The shearing effect, that is, the stirring rate, is the key to affecting the particle size of the resulting proppant [18]. The configuration of the emulsion was carried out based on the type of the selected emulsifier, and the particle size of the proppant obtained when the stirring rate was 150–400 rpm was evaluated. The evaluation results are shown in Figure 7.

It can be seen from the evaluation results that the particle size of the obtained proppant decreases with the increase in the stirring speed. When the stirring speed is 150 rpm, the particle size of the obtained proppant is mainly distributed in 4.5 mm. When the stirring speed is increased to 200, 250, 300, 350 and 400 rpm, the particle size of the obtained proppant is mainly distributed in 3 mm, 2–2.5 mm, 2 mm, 1 mm and 0.5 mm, respectively. To prevent the embedding of the obtained proppant in the NGH reservoir, a large-size proppant is required to support the reservoir, so the stirring speed is selected at 150–300 rpm.

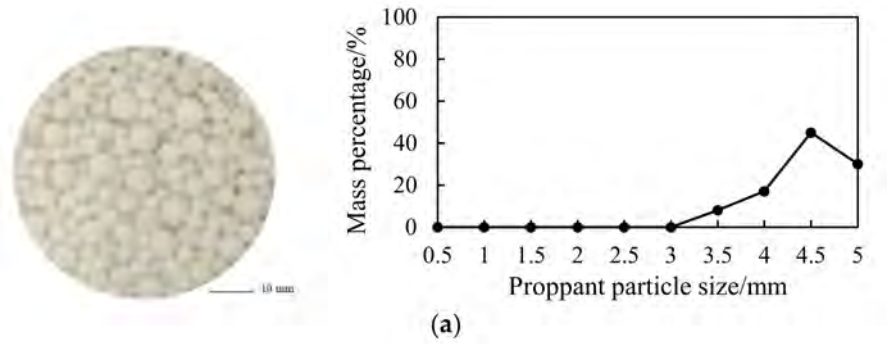

Figure 7. *Cont.*

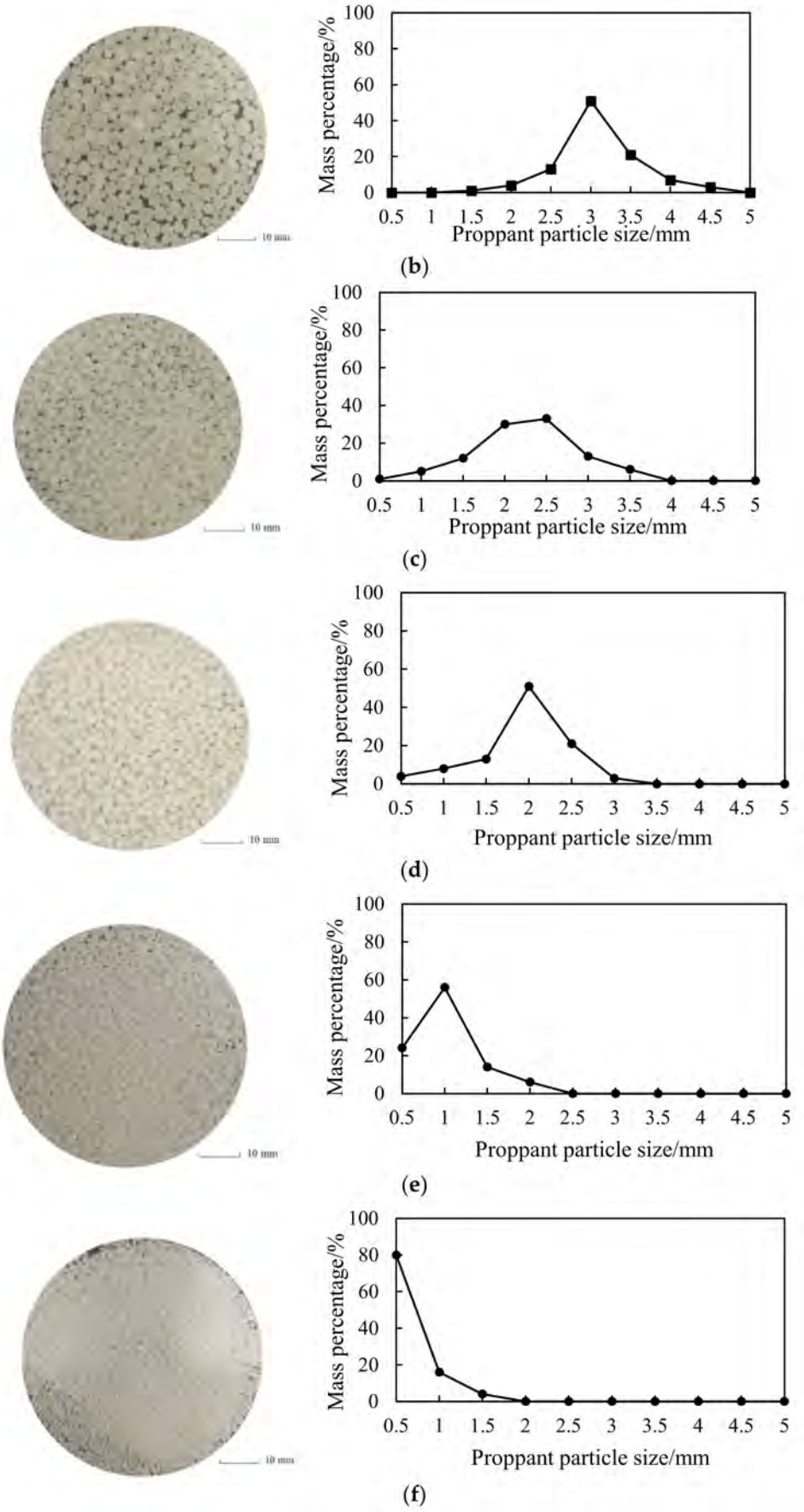

Figure 7. Proppant morphology and particle size distribution at different stirring speeds. ((**a**–**f**) are proppants obtained at stirring speeds of 150, 200, 250, 300, 350 and 400 rpm, respectively.)

2.6. Optimization of Emulsification Process

In the experiment, the viscosity of the phase change proppant increased during the curing process, and the cementation between particles occurred easily. For Pickering emulsions, the emulsion droplet surface does not require complete coverage of the emulsifier to remain stable [19]. To prevent the reduction in fracture permeability caused by the cementation between particles, the surface of the proppants in the emulsion phase is subjected to secondary adhesion treatment of large particles [20]. First, the surface morphology of the cured particles with the emulsifier dosage of 0.15%, 0.25%, 0.5%, 0.75% and 1% of the resin mass was evaluated by SEM, and the emulsifier coverage on the surface of the cured particles was obtained according to the evaluation results. For secondary adhesion of large particles while keeping the emulsion stable, select the emulsifier concentration with a coverage rate of more than 60% for the preparation of the emulsion. After the emulsion was initially stabilized, SiO_2 particles with a particle size of 100 μm and with a mass is 0.5% of the resin mass were added and stirred for 10 min to make secondary adhesion on the surface of the emulsion droplets, and then the resulting emulsion was allowed to stand until the resin was cured. Finally, the cementation between the cured proppants particles was evaluated to analyze the effect, and the surface microstructure of the particles was analyzed by SEM to analyze the mechanism of action. The evaluation results are shown in Table 2.

Table 2. Surface coverage of proppants obtained with different emulsifier concentrations.

Emulsifier Dosage/%	Particle Morphology	Particle Surface Morphology	Surface Coverage/%
0.15	No emulsion formed		
0.25	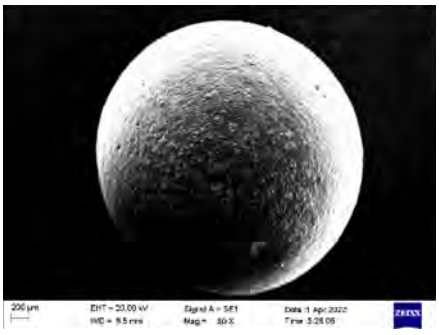	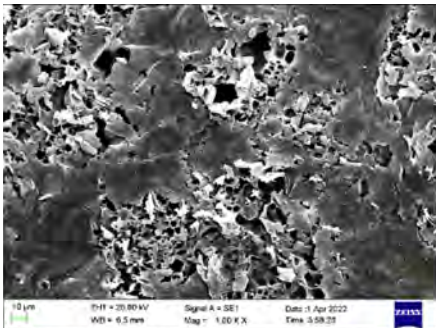	48%

Table 2. *Cont.*

Emulsifier Dosage/%	Particle Morphology	Particle Surface Morphology	Surface Coverage/%
0.5		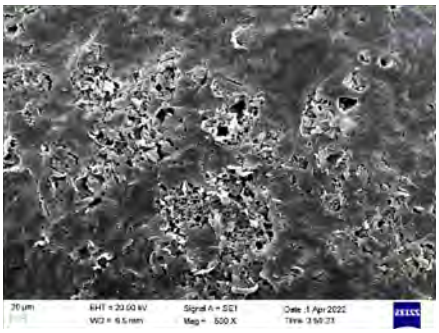	62%
0.75	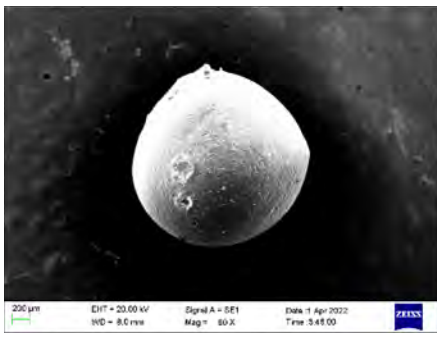	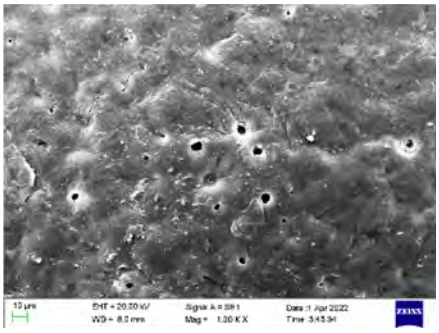	87%
1		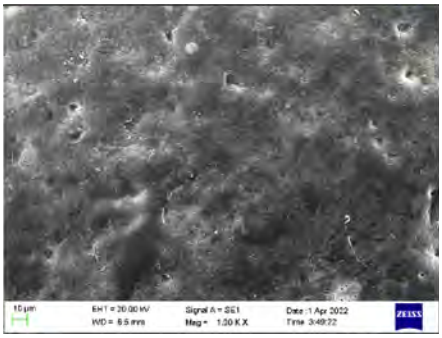	100%

It can be seen from the evaluation results in Table 2 that when the amount of emulsifier is 0.15% of the resin mass, no emulsion is formed because the amount of emulsifier is too low. When the amount of emulsifier increased to 0.25%, 0.5%, 0.75% and 1%, the surface emulsifier coverage obtained by curing the surface morphology of proppant particles was 48%, 63%, 87% and 100%, respectively. To maintain the stability of the obtained emulsion and carry out effective secondary adhesion, emulsion droplet surface coverage is 63%; that is, the amount of emulsifier that is 0.5% of the resin mass was selected. The obtained emulsion was subjected to secondary adhesion treatment. It can be seen from Figure 8 that SiO_2 particles with a particle size of 100 μm were effectively attached to the surface of the emulsion, and the cementation degree of the attached proppant during the curing process was significantly reduced (Figure 9). This is because surface particles of uneven size can induce changes in the contact pattern of emulsion droplets, and increase droplet spacing and spatial structure between droplets (Figure 10), thereby preventing the phenomenon of cementation from happening [21].

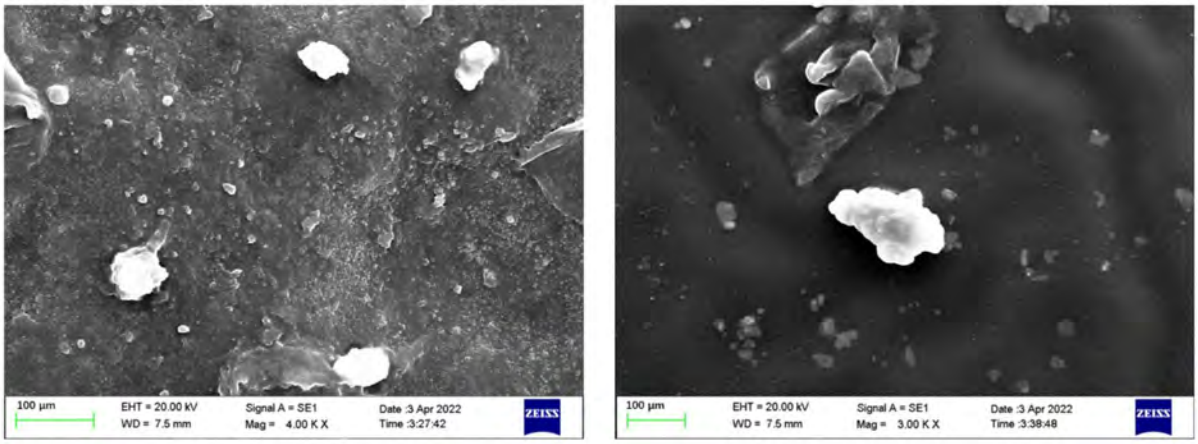

Figure 8. Adhesion of large particle size to the proppant's surface.

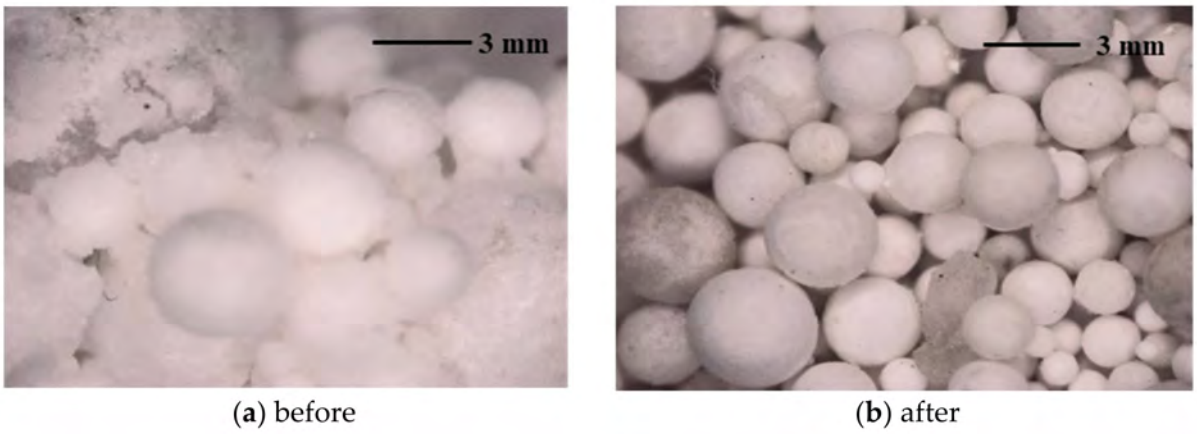

Figure 9. The cementation of proppant particles before and after the secondary adhesion.

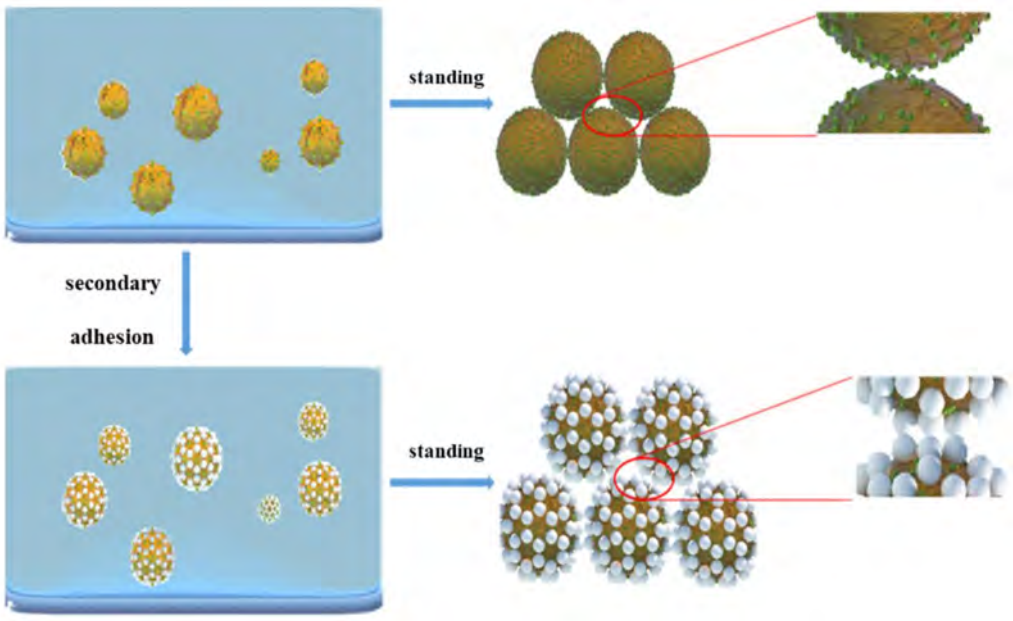

Figure 10. Changes in the packing shape of proppant particles after secondary attachment.

3. Evaluation Experiment of the Large-Size Resin Phase Change Proppants

3.1. Physical Property Evaluation

3.1.1. Proppant Morphology

The morphology of ceramsite, quartz sand and cured phase change proppant was analyzed with a VHX-6000 3D microscope system (Figure 11), and the morphology of different particles were compared.

Figure 11. VHX-6000 3D microscope system.

3.1.2. Compressive Strength

The uni-axial compressive strength of the cured proppants of different sizes was tested with the high-temperature and high-pressure rock test device, and the propping effects in the NGH reservoirs were analyzed.

3.2. Application Performance Evaluation

3.2.1. Analysis of Diversion Capacity and Proppant Embedment

To evaluate the diversion capacity and the degree of embedding of cured proppants in the marine NGH reservoirs, the rock sample with the physical properties close to those of the NGH reservoir was prepared. The rock sample was prepared with the quartz sand with the skeleton density of 2.65 $g \cdot cm^{-3}$ and the size of 0.089–0.104 mm as the medium particles. Hydrates are generated with the tetrahydrofuran. The clay and lime with a certain proportion was added to the quartz sand to simulate the weakly cemented clayey silt marine NGH reservoir. The processes of generating the rock samples are as follows [22]:

1. Mix montmorillonite, kaolinite and illite at a mass ratio of 7:2:1 as the clay component;
2. Add quartz sand, clay and lime at the mass ratio of 8:1:1;
3. Weigh a certain mass of the above-mentioned gravel into a beaker, and add the tetrahydrofuran solution of different masses into the beaker and stir the solution until the mixture is uniform;
4. Add the tetrahydrofuran-containing core sand and gravel into the abrasive tool in layers (Figure 12) and compact them layer by layer with a wooden rod. After filling, seal the abrasive tool to prevent volatilization, and let it stand for 7 days until the cement is cured.

Figure 12. Mold for making the NGH reservoir samples.

The triaxial shear of the in situ-generated NGH was test in the rock sample under the confining stress of 1 MPa, 3 MPa and 5 MPa and with the NGH content as 0 and a clay content of 10%. The physical properties of the prepared rock samples were compared with those of the marine NGH reservoirs. Subsequently, the prepared rock sample was ground into a rock slab with a length of 17.78 cm, a width of 3.81 cm and a thickness of 0.8–1 cm (Figure 13). Then, it was used to evaluate the short-term diversion capacity of proppant with different particle sizes compared with quartz sand proppant, and the embedding degree of proppant with different particle sizes and its effect on diversion capacity was evaluated [23]. The specific experimental scheme is shown in Table 3.

Figure 13. Morphology of rock slab.

Table 3. Experimental scheme of diversion capacity.

Proppant Sizes/mm	Proppant Type	Closing Pressure/MPa	Sand Laying Concentration/kg/m^2
4.5	Solidified phase change proppant Quartz sand proppant	0–20	10
3	Solidified phase change proppant Quartz sand proppant	0–20	10
2–2.5	Solidified phase change proppant Quartz sand proppant	0–20	10
0.5–1	Solidified phase change proppant Quartz sand proppant	0–20	10

3.2.2. Migration Ability

Experiment

The migration capabilities of the same-size quartz sand proppants and the emulsion phase change proppants under the same conditions were compared in the visual migration and deposition device (Figure 14), and the migration capacity of the emulsion-phase proppants in the liquids of different viscosities was evaluated. The experiment scheme is listed in Table 4.

Figure 14. Visual proppant migration test device.

Table 4. Proppant migration and sedimentation test scheme.

Proppant Types	Displacement/(m^3/h)	Proppant Concentration/%	Frac Fluid Viscosity/mPa·s
Quartz sand proppant	5.4	10	1
Emulsion-phase proppant	5.4	10	1
Emulsion-phase proppant	5.4	10	15
Emulsion-phase proppant	5.4	10	25

Simulation

To assess the transport capacity of self-generated proppant in real fractures, a proppant-transport simulation model was developed using COMSOL version 5.5. Since there is no actual fracturing practice for a hydrate reservoir, the fracture length in the simulation is set as 50 m based on the fracture length of the oil and gas reservoir. The transport capacity of quartz sand proppant and emulsion phase change proppant at 1 mPa·s carrying fluid viscosity and the transport capacity of emulsion phase change proppant at 1 mPa·s and 15 mPa·s carrying fluid viscosity were compared by simulation. The key boundary conditions are shown in Figure 15.

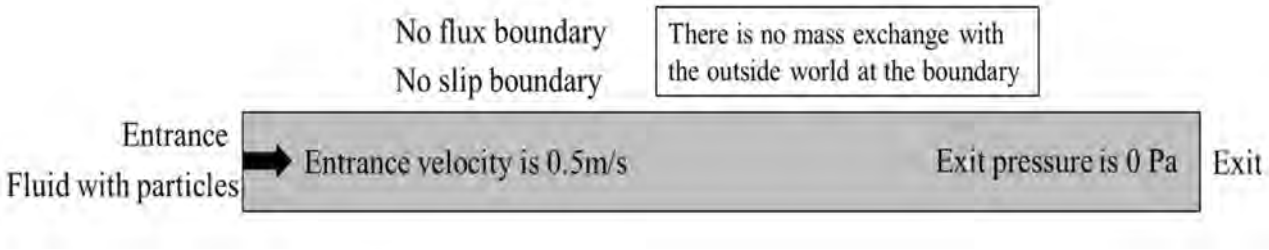

Figure 15. The boundary conditions of the model.

4. Results and Discussions

4.1. Physical Property Evaluation Results

4.1.1. Proppant Morphology

The regular structure and surface morphology of proppants particles are the basis for the formation of a high-conductivity seepage channel after they are laid. The morphology of quartz sand, ceramsite and cured resin proppant are compared, as shown in Figure 16.

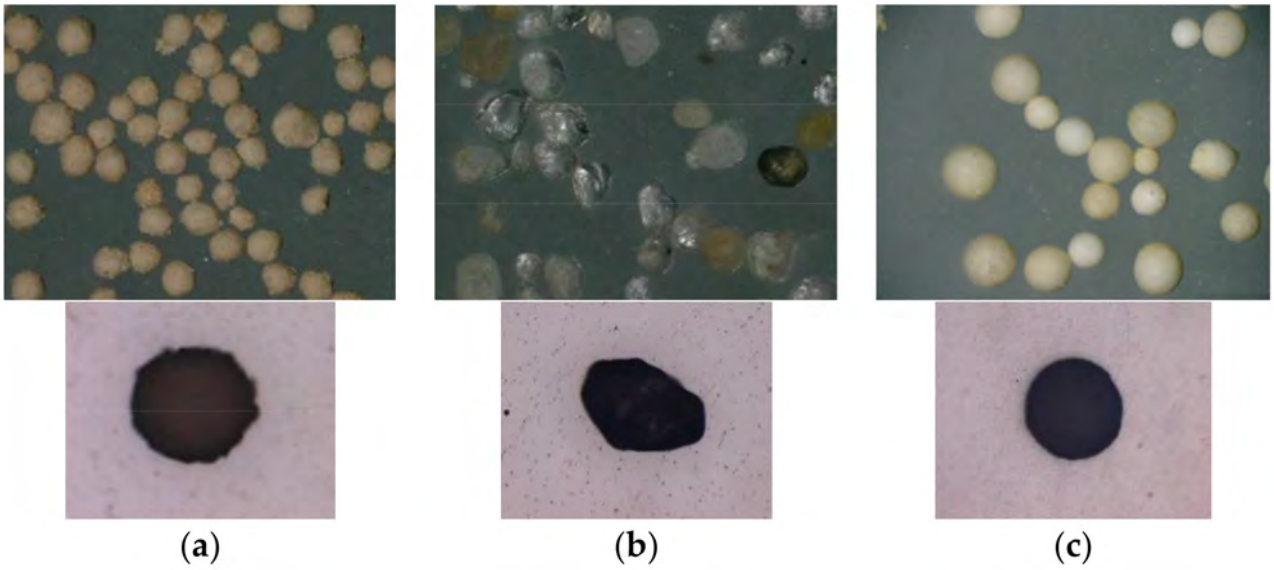

Figure 16. Morphology of different proppant particles. ((**a**–**c**) are the morphology of ceramsite proppant, quartz sand proppant and solidified phase change proppant.)

Compared with the ceramsite and quartz sand, the cured phase change proppants have more regular structure and surface morphology. Therefore, the solidified phase change proppants have a larger spatial structure in the stacking state, and their stacking state changes less under the action of closing pressure, which can maintain a better conductivity [24].

4.1.2. Compressive Strength

The good compressive strength of proppant particles is the basis for maintaining the stability of the seepage channel in the reservoir with a certain closing pressure. The compressive strength of different sizes of proppant particles after curing are shown in Figure 17.

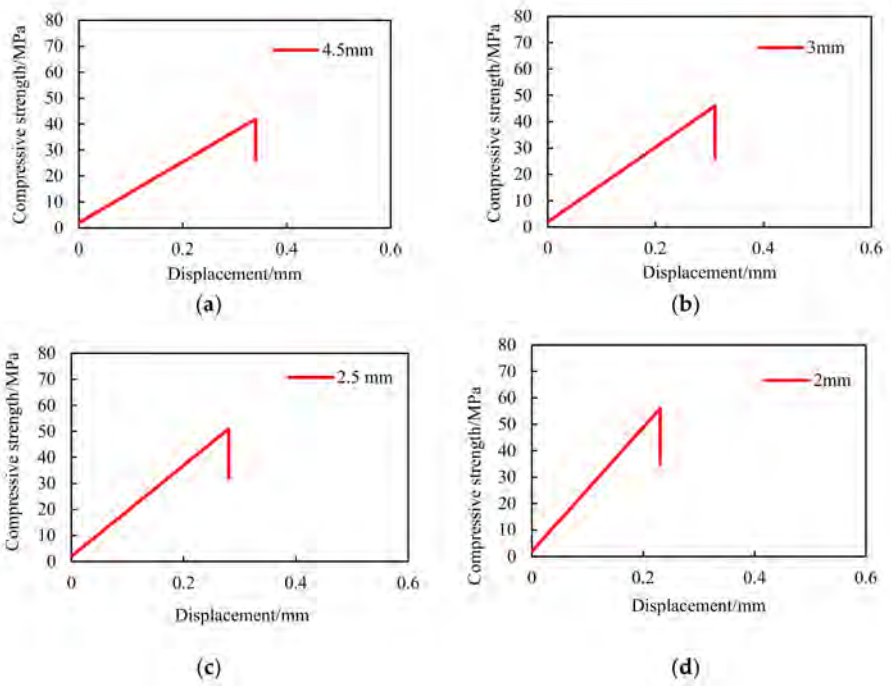

Figure 17. Compressive strength of cured proppants with different sizes. ((**a**–**d**) are the compressive strengths of proppants with particle sizes of 4.5 mm, 3 mm, 2.5 mm and 2 mm, respectively.)

From the evaluation results, the compressive strength of the proppant increases with the decrease in particle size. The compressive strengths of proppant particles with particle sizes of 4.5 mm, 3 mm, 2.5 mm and 2 mm are 42 MPa, 46 MPa, 51 MPa, and 56 MPa, respectively. The marine NGH reservoirs are buried in shallow depth, and the closure stress is usually not higher than 20 MPa. Thus, the strength of the obtained large-size phase change proppant meets the needs of propping the fracture in the NGH reservoirs.

4.2. Application Performance Evaluation Results

4.2.1. Diversion Capacity and Proppant Embedment Evaluation Results

a. Mechanical characteristics of the NGH reservoir rock samples

Triaxial shear test was performed on the marine NGH reservoir sample with 10% clay content and 0% NGH content. The stress–strain curve and Mohr circle are shown in Figure 18.

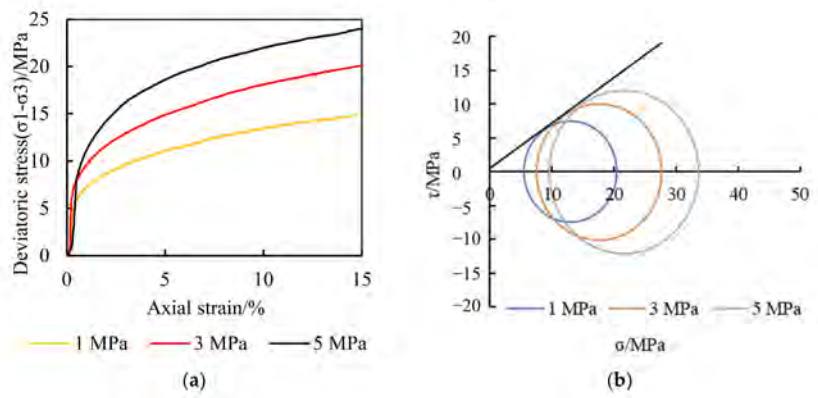

Figure 18. Stress-strain curve and Mohr circle of rock samples of the marine NGH reservoir. (**a**) is the stress-strain curve of rock samples; (**b**) is the mohr circle of rock samples.

According to the stress–strain curve of the marine NGH rock sample, the shear strengths of the rock sample are 14.9 MPa, 20.1 MPa and 24.1 MPa under the effective confining stress of 1 MPa, 3 MPa and 5 MPa, respectively. The stress-strain curves have no obvious peak, indicating that the rock sample shows plastic properties. According to the Mohr's circle, the cohesion and internal friction angle of the NGH sediment core are 1.37 MPa and 33.03°. Due to the characteristics of shallow burial depth, weak formation compaction and weak cementation of marine NGH reservoir, the stress–strain curve of the rock sample is plastic as a whole, which is in line with the actual situation of a marine NGH reservoir [25].

b. Evaluation results of the proppant diversion capacity

The experimental results of diversion capacity of solidified resin proppant and quartz sand proppant with the same particle size are shown in Figure 19.

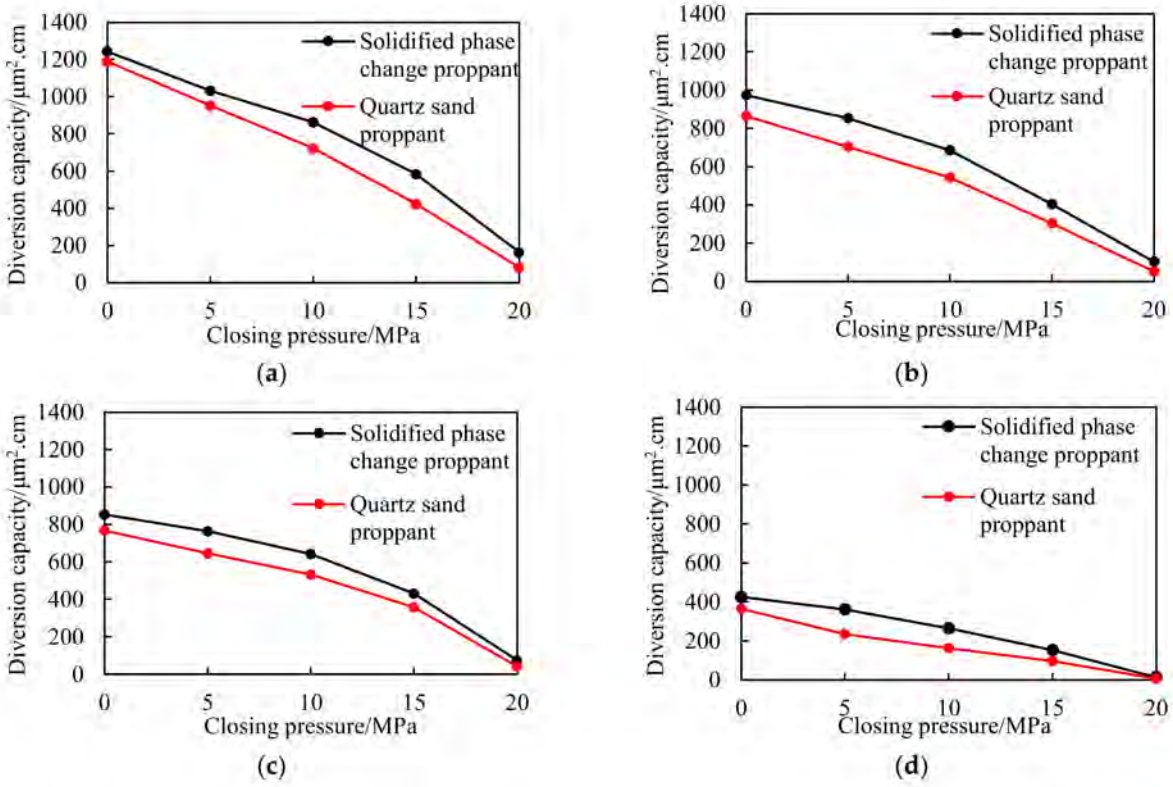

Figure 19. Evaluation results of diversion capacity of solidified phase change proppant and quartz sand proppant with the same particle size. ((**a**–**d**) are the evaluation results of the diversion capacity of solidified phase change proppant and quartz sand proppant with particle sizes of 4.5 mm, 3 mm, 2–2.5 mm and 0.5−1 mm, respectively.)

It can be obtained from the evaluation that because of the embedding of proppant in the marine NGH reservoir, its diversion capacity decreases significantly with the increase in closing pressure (Figure 20). When the closing pressure of the solidified phase change proppants with particle sizes of 4.5 mm, 3 mm, 2–2.5 mm and 0.5–1 mm was increased from 0 MPa to 20 MPa, their diversion capacity decreased from 1243 μm²·cm, 973 μm²·cm, 853 μm²·cm and 426 μm²·cm to 164 μm²·cm, 103 μm²·cm, 74 μm²·cm and 14 μm²·cm, respectively. Among them, proppants with particle sizes of 4.5 mm, 3 mm and 2–2.5 mm can meet the requirements of forming effective seepage channels, although the conductivity of proppants is greatly reduced because of the embedding of proppants [26]. Compared with the quartz sand proppants with the same particle size, the solidified phase change proppants have higher diversion capacity. This is because the solidified phase change

proppants have a more regular morphology than the quartz sand proppants, so its packing morphology changes less when subjected to closing pressure and the degree of embedding in the marine NGH reservoir is lower.

Figure 20. Embedding of solidified phase change proppant on the surface of rock slab.

c. Analysis results of the influence of proppants embedding in branch cracks and micro cracks

For distal fractures and branch fractures, large-sized proppants are difficult to enter in large quantities because of the small fracture size. Therefore, the proppants are usually laid in a single layer in distal fractures and branch fractures [27]. To evaluate the effect of embedding in the single-layer laying, small-size embedding experiments of individual proppant particles were carried out. The embedding degree of cured proppants of different sizes under the closing pressure of 20 MPa in the marine NGH reservoir rock samples was evaluated, as shown in Figure 21.

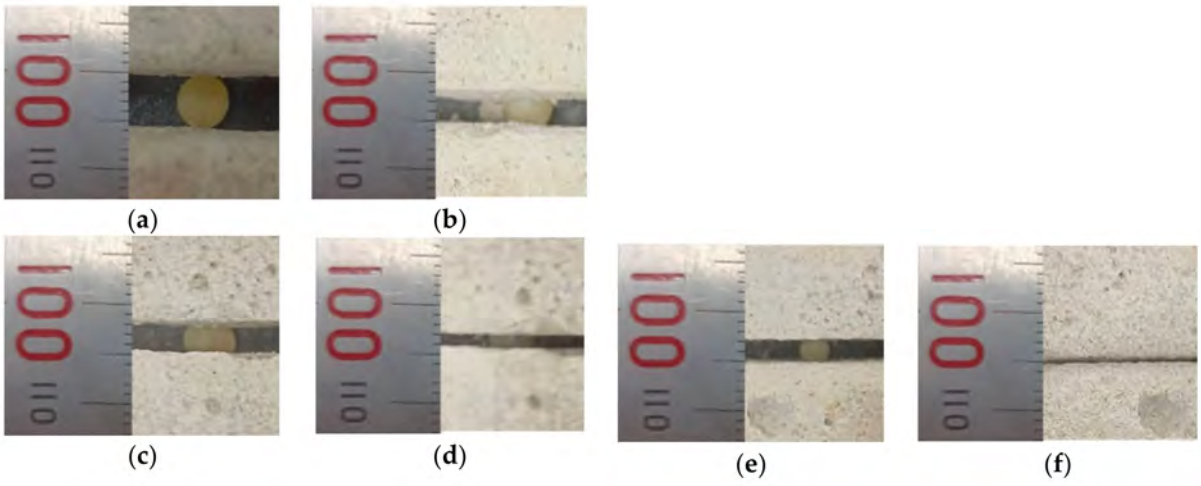

Figure 21. Experimental results of small-size embedding of medium-size proppant particles. ((**a**,**b**) are the embedding degree of proppants with a size of 4.5 mm in the fracture under and not under the closure stress; (**c**,**d**) are the embedding degree of proppants with a size of 3 mm in the fracture under and not under the closure stress; (**e**,**f**) are the embedding degree of proppants with a size of 2.5 mm in the fracture under and not under the closure stress).

According to Figure 21, proppants are embedded seriously in the marine NGH reservoirs, the proppants with a size of less than 2.5 mm are almost embedded, and an effective conduction channel cannot be formed. The 4.5 mm and 3 mm resin proppants still provide the 2.5 mm and 1 mm conduction channels after embedding, which can meet the mining needs of the marine NGH reservoirs. Therefore, according to the evaluation results, further optimized, the suitable proppant particle size is 3–4.5 mm, and the mixing rate is further optimized to 150–200 rpm. The obtained large-particle-size phase change

proppants can simultaneously support the main fractures, distal fractures and branch fractures generated after fracturing and meet the needs for the development of marine NGH reservoirs fracturing.

4.2.2. Migration Ability Evaluation Results

Experiment

a. The migration capacity of the quartz sand and the emulsion large-particle-size phase change proppants is compared, as shown in Figure 22.

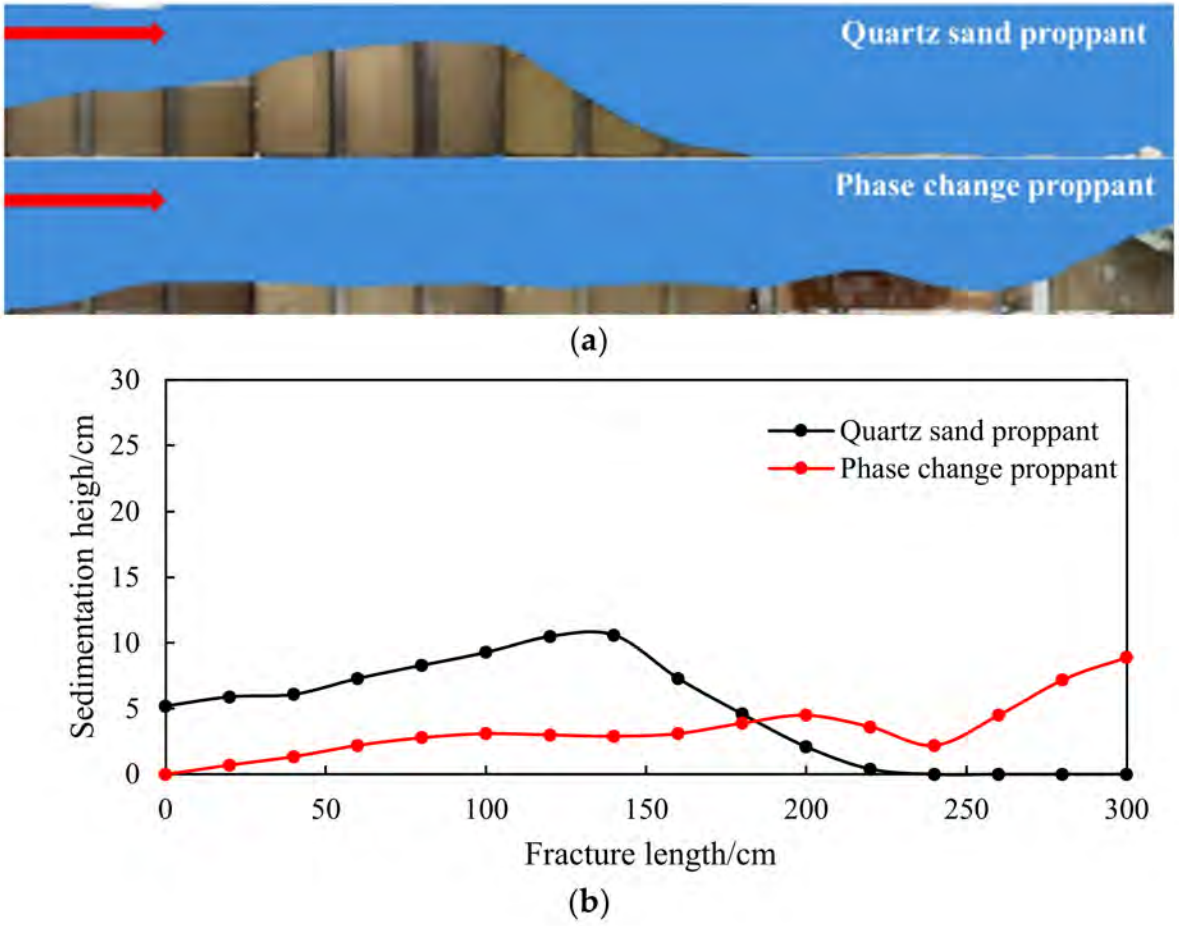

Figure 22. Experimental results and data of proppant migration. (**a**) is the proppant migration experimental results; (**b**) is the data of experimental results.

From the results of quartz sand migration experiment with the same size and emulsion phase resin phase change proppant with a sand ratio of 10% under the conditions that the viscosity of carrier fluid is 1 mPa·s and the displacement is 5.4 m^3/h. It can be seen that the quartz sand proppant completely settles in the area near the well and cannot be effectively transported, while the same-size emulsion-phase resin phase change proppant can be uniformly laid in the fracture. This is due to the lower density of the resin and the droplet friction reduction because of the high sphericity of the emulsion droplets. Therefore, the migration ability of the obtained emulsion-phase resin phase change proppant is significantly better than the commonly used quartz sand proppant and can be effectively transported by the low-viscosity carrying fluid.

b. The comparison results of the migration capacity of the emulsion-phase resin phase change proppant in the carrying fluid with different viscosities are shown in Figure 23.

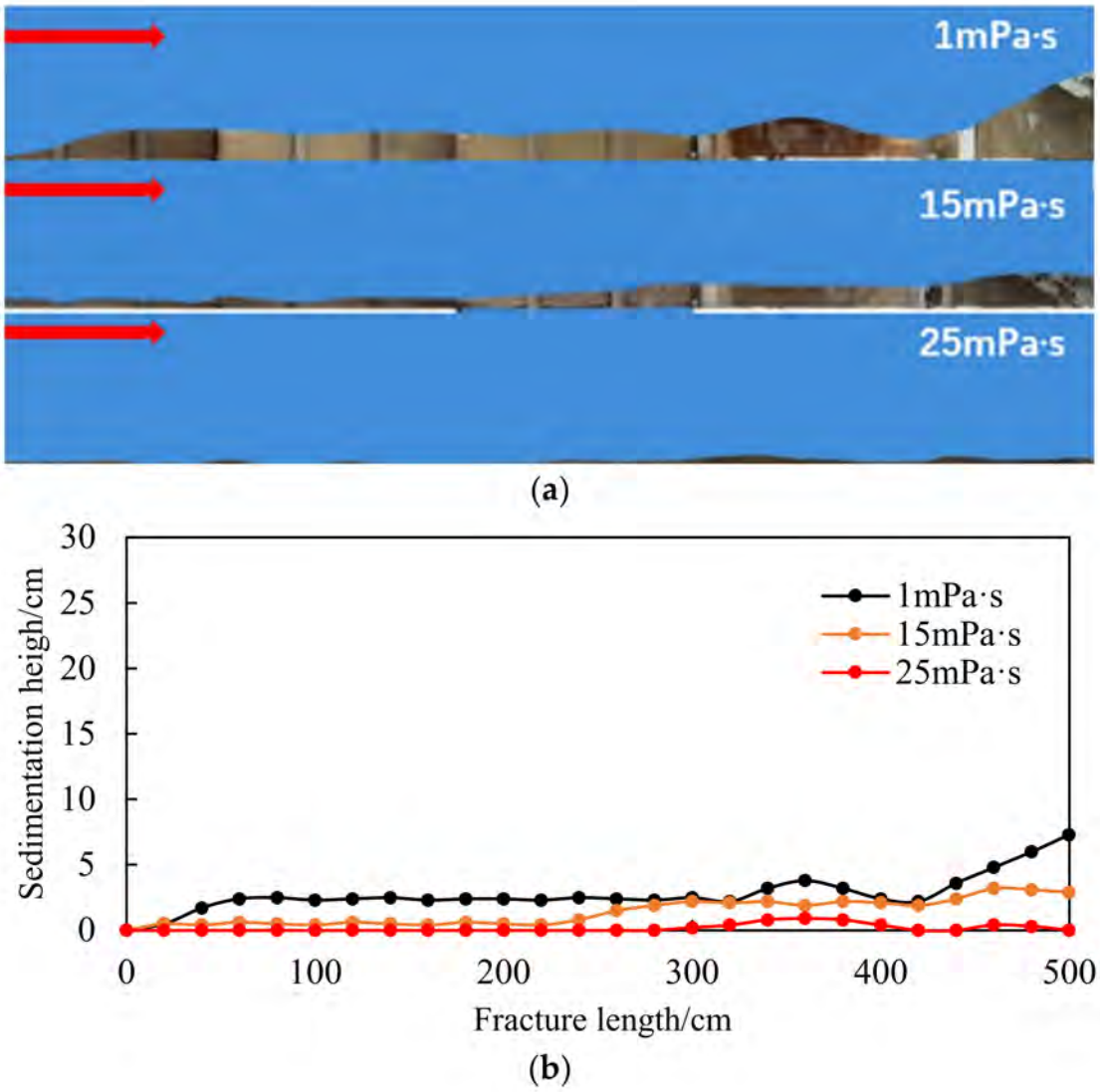

Figure 23. Experimental results and data results of migration of emulsion-phase resin phase change proppant in carrying fluids with different viscosities. (**a**) is the proppant migration experimental results; (**b**) is the data of experimental results.

According to the experiment results of proppant migration, the carrying-fluid viscosity has a significant effect on the proppant migration capability. The high-viscosity fluid provides better suspension capability for the emulsion droplets, and the migration capacity of the proppant increases significantly with an increase in the carrying-fluid viscosity. With a carrying-fluid viscosity of 1 mPa·s, the phase change proppants can be placed evenly within the fracture. When the viscosity of the carrying liquid rises to 15 mPa·s, the volume of deposited proppants is reduced significantly. When the viscosity of the carrying liquid rises to 25 mPa·s, the proppants in the emulsion phase hardly settle down. In the field application, the propping effects in the fracture in the NGH reservoirs can be improved by controlling the fluid viscosity according to the length of the fracture and the location of the required propping position.

Simulation

The simulation results are shown in Figure 24.

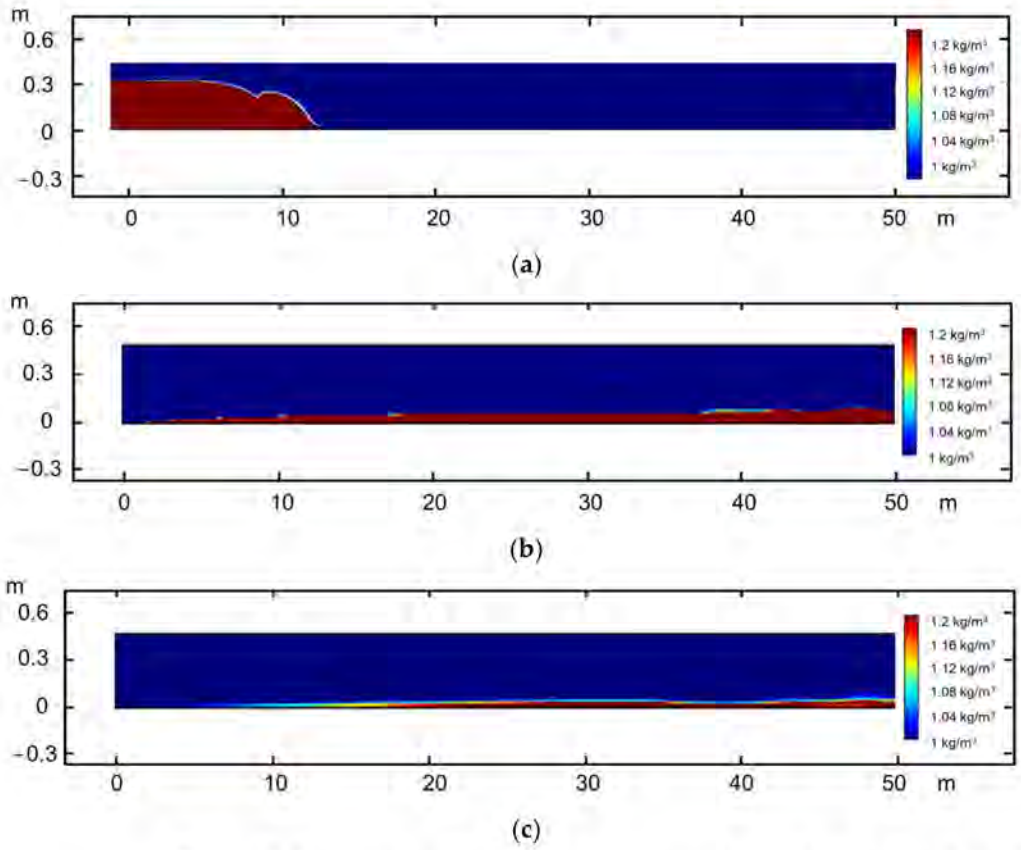

Figure 24. Simulation results of proppant transport capacity in near-real-size fractures. ((**a**) is the simulation result of the migration capability of the quartz sand proppants at a viscosity of 1 mPa·s; (**b**,**c**) are the simulation result of the migration capability of the emulsion phase change proppant at the viscosity of 1 mPa·s and 15 mPa·s).

From the simulation results, we found that the simulation and the experiment showed the same pattern. The quartz sand proppant is difficult to be effectively carried by low-viscosity carrying fluids, and almost all of it settles in the immediate vicinity of the wellbore. The emulsion-phase change proppants can be effectively carried to the distal fracture by the low-viscosity liquid, and no obvious settlement phenomenon occurs when the liquid viscosity increases. The simulation results show that the emulsion-phase change proppants have better transport capacity than quartz sand proppants and can effectively transport to the distal fracture in the real fracture size.

5. Conclusions

In this study, we developed the large-size phase change proppants by preparing the high-efficiency low-temperature curing agent and emulsifying the epoxy resin and curing agent system, and resolved the problems of serious embedding of small proppants and poor migration capability of large proppants in the NGH reservoirs. The proppants' performances were evaluated. The conclusions are obtained as follows.

- Polythiol curing agent was generated by adding the glycerol and mercaptopropionic acid with a molar ratio of 1:3 as the reactive monomer and through esterification with the concentrated sulfuric acid as the acid catalyst and dehydrating agent. The polythiol curing agent is compounded with the amine agent and the adduct of diethylene triamine and butyl glycidyl ether with a ratio of 6:4. The curing time is reduced to less than 40 min under a humid environment at a temperature of 5 °C.
- Large proppants with uniform size can be obtained by adding 0.05 μm SiO_2 particles as the emulsifier with the dosage is 0.5% of the resin mass and the ratio of curing

system to emulsifier solution as 5:1, with the 20% ethanol as the diluent, and stirring the solution at the rate of 150–200 rpm. The particle size of the obtained proppants is greater than 3 mm. The 100 μm SiO_2 particles with the dosage of 0.5% of the resin mass were added for secondary adhesion, which can prevent particle aggregation during the standing of proppants.

- The solidified large-particle-size phase change proppants have more regular morphology than quartz sand and ceramsite, and the compressive strength of the particles decreases with an increase in the size. The compressive strength of 4.5 mm proppants reaches 42 MPa, which meets the needs in the development of NGH reservoirs.
- In the seriously embedded NGH reservoirs, the proppant with particle sizes greater than 3 mm can still maintain good conductivity under the closing pressure of 20 MPa and can also effectively support the branch fracture of the distal fracture. The migration capacity of liquid proppants is much higher than that of solid proppants with the same size, and the migration capacity increases significantly with an increase in the carrying fluid viscosity. The propping position can be controlled accurately by controlling the viscosity of the carrying fluid.

Author Contributions: Conceptualization, Z.Q.; writing—review and editing, J.F.; software, T.G.; formal analysis, J.H.; resources, M.W.; methodology, X.L. All authors have read and agreed to the published version of the manuscript.

Funding: This research was funded by [National Natural Science Foundation of China] grant number [52074332], [Shandong Provincial Science Fund for Excellent Young Scholars] grant number [ZR2020YQ36], [National Natural Science Foundation of China] grant number [52204024] and [China Postdoctoral Science Foundation] grant number [2022M710225].

Institutional Review Board Statement: Not applicable.

Informed Consent Statement: Not applicable.

Conflicts of Interest: The authors declare no conflict of interest.

References

1. Liu, X.; Zhang, W.; Qu, Z.; Guo, T.; Sun, Y.; Rabiei, M.; Cao, Q. Feasibility evaluation of hydraulic fracturing in hydrate bearing sediments based on analytic hierarchy process-entropy method. *J. Nat. Gas Sci. Eng.* **2020**, *81*, 103434. [CrossRef]
2. Feng, Y.; Chen, L.; Suzuki, A.; Kogawa, T.; Okajima, J.; Komiya, A.; Maruyama, S. Enhancement of gas production from methane hydrate reservoirs by the combination of hydraulic fracturing and depressurization method. *Energy Convers. Manag.* **2019**, *184*, 194–204. [CrossRef]
3. Shi, S.S.; Chen, X.Z.; Ma, J. Natural Gas Hydrate Reservoir Classification and Characterization in the Well W19 of Shenhu Sea Area, Northern South China Sea. *Spec. Oil Gas Res.* **2019**, *26*, 24–29.
4. Draper, E.R.; Adams, D.J. Low-molecular-weight gels: The state of the art. *Chem* **2017**, *3*, 390–410. [CrossRef]
5. Wang, T.Y.; Shen, Z.C.; Liu, M.H. Supramolecular polymer gels. *Acta Polym. Sin.* **2017**, *1*, 50–62.
6. Pei, Y.; Zhao, P.; Zhou, H.; Li, D.; Liao, X.; Shao, L.; Zhang, S.; Tian, F.; Zhao, Y.; Zhang, N.; et al. Development and latest research advances of self-propping fracturing technology. *SPE J.* **2021**, *26*, 281–292. [CrossRef]
7. Kang, B.U.; Jho, J.Y.; Kim, J.; Lee, S.S.; Park, M.; Lim, S.; Choe, C.R. Effect of molecular weight between crosslinks on the fracture behavior of rebber-toughened epoxy adhesives. *J. Appl. Polym. Sci.* **2001**, *79*, 38–48. [CrossRef]
8. Zhao, L.; Chen, Y.; Du, J.; Liu, P.; Li, N.; Luo, Z.; Zhang, C.; Huang, F. Experimental studyon a new type of self-propping fracturing technology. *Energy* **2019**, *183*, 249–261. [CrossRef]
9. Luo, Z.; Zhang, N.; Zhao, L.; Pei, Y.; Liu, P.; Li, N. Thermore-sponsive in situ generated proppant based on liquid–solid transition of a supramolecular self-propping frac fluid. *Energy Fuels* **2019**, *33*, 10659–10666.
10. Chen, L.; Chen, Q.; Xu, L. Preparation and volume stability of polythiol/amine compound modified bisphenol a epoxy resin. *Colloids Polym.* **2015**, *33*, 159–161. [CrossRef]
11. Zhou, S.; Chen, W.; Li, Q. Green mining technology for solid-state sulphurization of deep-water and shallow natural gas hydrates. *China Offshore Oil Gas* **2014**, *26*, 1–7.
12. Zhu, Z.; Yang, J.; Xu, X. Study on reducing viscosity of crude oil emulsions by Pickering emulsion from mineral powder. *Mod. Chem. Ind.* **2019**, *39*, 141–145.
13. Guo, T.; Wang, X.; Li, Z.; Gong, F.; Lin, Q.; Qu, Z.; Lv, W.; Tian, Q.; Xie, Z. Numerical simulation study on fracture propagation of zipper and synchronous fracturing in hydrogen energy development. *Int. J. Hydrogen Energy* **2018**, *44*, 5270–5285. [CrossRef]

14. Ritzenthaler, S.; Court, F.; David, L.; Girard-Reydet, E.; Leibler, L.; Pascault, J.P. ABC triblock copolymers/epoxy-diamine blends. 1. Keys to achieve nanostructured thermosets. *Macromolecules* **2002**, *35*, 6245–6254. [CrossRef]
15. Horozov, T.S.; Binks, B.R.; Gottschalk-Gaudig, T. Effect of electrolyte in silicone oil-in-water emulsions stabilised by fumed silica particles. *Phys. Chem. Chem. Phys.* **2007**, *9*, 6398–6404. [CrossRef]
16. Lee, G.J.; Son, H.A.; Cho, J.W.; Choi, S.K.; Kim, H.T.; Kim, J.W. Stabilization of pickering emulsions by generating complex colloidal layers at liquid-liquid interfaces. *J. Colloid Interface Sci.* **2014**, *413*, 100–105. [CrossRef] [PubMed]
17. Xia, T.; Xue, C.; Wei, Z. Physicochemical characteristics, applications and research trends of edible Pickering emulsions. *Trends Food Sci. Technol.* **2021**, *107*, 1–15. [CrossRef]
18. Wang, Y.Q.; Liu, S.; Liu, Z.P. Water isolation and protective performance of waterborne graphene-dopes epoxy coating. *Electroplat. Finish.* **2015**, *34*, 314–319.
19. Ortiz, D.G.; Pochat-Bohatier, C.; Cambedouzou, J.; Bechelany, M.; Miele, P. Current trends in pickering emulsions: Particle morphology and applications. *Engineering* **2020**, *6*, 468–482. [CrossRef]
20. Miao, C.; Atifi, S.; Hamad, W.Y. Properties and stabilization mechanism of oil-in-water Pickering emulsions stabilized by cellulose filaments. *Carbohydr. Polym.* **2020**, *248*, 116775. [CrossRef]
21. Khedr, A.; Striolo, A. Self-assembly of mono- and poly-dispersed nanoparticles on emulsion droplets: Antagonistic vs. synergistic effects as a function of particle size. *Phys. Chem. Chem. Phys.* **2020**, *22*, 22662–22673. [CrossRef]
22. Liu, X.; Guo, T.; Qu, Z. Feasibility evaluation model and application of hydraulic fracturing in hydrate reservoir. *J. Cent. South Univ.* **2022**, *53*, 1058–1068.
23. Guo, T.; Gong, F.; Lin, X.; Lin, Q.; Wang, X. Experimental investigation on damage mechanism of guar gum fracturing fluid to low-permeability reservoir based on nuclear magnetic resonance. *J. Energy Resour. Technol.* **2018**, *140*, 072906. [CrossRef]
24. Zhu, W.; Liu, Q.; Yue, M.; Zhang, L. Calculation of fracture conductivity considering proppant influence and simulation of proppant transport in fracture. *Chem. Eng. Oil Gas* **2019**, *48*, 75–78. [CrossRef]
25. Koh, D.Y.; Kang, H.; Lee, J.W.; Park, Y.; Kim, S.J.; Lee, J.; Lee, J.Y.; Lee, H. Energy-efficient natural gas hydrate production using gas exchange. *Appl. Energy* **2016**, *162*, 114–130. [CrossRef]
26. Chen, D.; Shi, J.Q.; Durucan, S.; Korre, A. Gas and water relative permeability in different coals: Model match and new insights. *Int. J. Coal Geol.* **2014**, *122*, 37–49. [CrossRef]
27. Liu, X.; Qu, Z.; Guo, T.; Tian, Q.; Lv, W.; Xie, Z.; Chu, C. An innovative technology of directional propagation of hydraulic fracture guided by radial holes in fossil hydrogen energy development. *Int. J. Hydrogen Energy* **2018**, *44*, 5286–5302. [CrossRef]